

Conjugate points in stadium and circle billiards

W. A. Lin and R. V. Jensen

Department of Physics, Wesleyan University, Middletown, Connecticut 06459

(Received 26 June 1997)

In the semiclassical approximation of the Green's function, the Maslov index is obtained by counting the number of conjugate points along classical orbits. We prove that if an orbit starts from the boundary of a stadium or a circle billiard, a conjugate point can never land on the boundary and that there is a conjugate point after a bounce off the boundary if and only if the bounce occurs on a curved side. We demonstrate exceptions to this simple rule when the orbit starts from the interior of the billiard domain. These results are useful for semiclassical calculations involving stadium and circle billiards. [S1063-651X(97)05711-5]

PACS number(s): 05.45.+b, 03.65.Sq, 31.15.Gy, 02.90.+p

I. INTRODUCTION

Semiclassical approximations of quantum mechanics provide a link between classical orbits and quantum interference phenomena. One of the important questions is how chaos manifests itself in quantum mechanics. Stadium and circle billiards are paradigmatic systems for pursuing this question. The underlying difference in the classical dynamics, chaotic vs regular, has direct consequences in recent experiments on quantum dot transport [1–6]. Semiclassical approximations have been employed to study various aspects of these billiard systems [1,4,7–12]. One of the quantities frequently used in these studies is the semiclassical Green's function [13,14]. It is expressed in terms of a sum over classical orbits at constant energy, with each contributing orbit carrying an amplitude and a phase. Conjugate points are locations along the orbit where the amplitude diverges (see Ref. [13] for a more detailed definition of a conjugate point). The phase depends on the Maslov index, which requires the knowledge of the number of conjugate points encountered by the orbit. The calculation of the Maslov index is a major task in semiclassical calculations.

In this paper we derive a simple rule for counting the conjugate points when orbits begin on the boundary of a stadium or a circle billiard. The proof of the rule will be based on the monodromy matrix of a convex billiard in Birkhoff coordinates [15].

Consider a general (hard-wall) convex billiard; one can uniquely specify a classical orbit in terms of the Birkhoff coordinates (s, p_s) [16]. The position coordinate s is defined to be the length along the billiard boundary from some reference point to the bounce point and can be chosen to be increasing in a counterclockwise fashion. The conjugate momentum variable $p_s = p \cos \theta$ is the tangential momentum of the billiard along the boundary at the bounce point [17], where θ is the angle of the reflected ray from the tangent (pointing in the direction of increasing s) to the boundary at the bounce point.

For an orbit that begins on the boundary of a general convex billiard, we define the monodromy matrix after n bounces as $M^{(n)} = \prod_{j=1}^n \hat{M}_j$, where the monodromy matrix for the j th step from the $(j-1)$ th bounce point to the j th bounce point is given by [15]

$$\hat{M}_j = \begin{pmatrix} \frac{l_j/R_{j-1} - \sin \theta_{j-1}}{\sin \theta_j} & \frac{-l_j}{\sin \theta_{j-1} \sin \theta_j} \\ \frac{\sin \theta_{j-1}}{R_j} + \frac{\sin \theta_j}{R_{j-1}} - \frac{l_j}{R_{j-1}R_j} & \frac{l_j/R_j - \sin \theta_j}{\sin \theta_{j-1}} \end{pmatrix} \quad (1)$$

for unit momentum $p = 1$, where R_j is the radius of curvature of the boundary at the j th bounce point, θ_j is θ at the j th bounce point (the starting point is referred to as the zeroth bounce and the ray emerging from the starting point is considered as a reflected ray even though no actual bounce off the wall occurs), and l_j is the distance between the two bounces.

In terms of the Birkhoff coordinates, the semiclassical Green's function for a general convex billiard can be written as [13,14,18]

$$G_{\mathcal{E}}^c(s'', s') = \frac{2\pi}{(2\pi i \hbar)^{3/2}} \sum_{u(s', s'')} \sqrt{|D_u|} \exp \left[\frac{i}{\hbar} S_u - i \frac{\pi}{2} \mu_u \right], \quad (2)$$

where the summation is over all classical paths u that begin at s' and end at s'' at energy \mathcal{E} , S_u is the action $\int_{s'}^{s''} \mathbf{p} \cdot d\mathbf{q}$ of the path, $|D_u| = |\partial^2 S_u / \partial s'' \partial s'| / |\dot{z}' \dot{z}''|$, \dot{z}' (\dot{z}'') is the longitudinal velocity of the trajectory at the starting (ending) point, and μ_u is the Maslov index. The Maslov index μ_u is determined by the number of conjugate points encountered along the path plus twice the number of bounces off the billiard boundary (assuming a hard wall) [8]. D_u diverges at conjugate points [8], which makes the semiclassical approximation invalid. To have a good semiclassical approximation, it is essential that the end points (s'') of all the orbits included in the sum are away from conjugate points. Thus knowledge about exact locations of the conjugate points will help us avoid bad semiclassical approximations.

Based on the monodromy matrix, we prove in Sec. II that if an orbit starts from the boundary of a stadium, (i) a conjugate point can never land on the boundary and (ii) there is a conjugate point after a bounce if and only if the bounce occurs on a curved side. We show in Sec. III that these simple rules are violated if the orbit starts from the interior of the billiard domain. A condition under which a conjugate

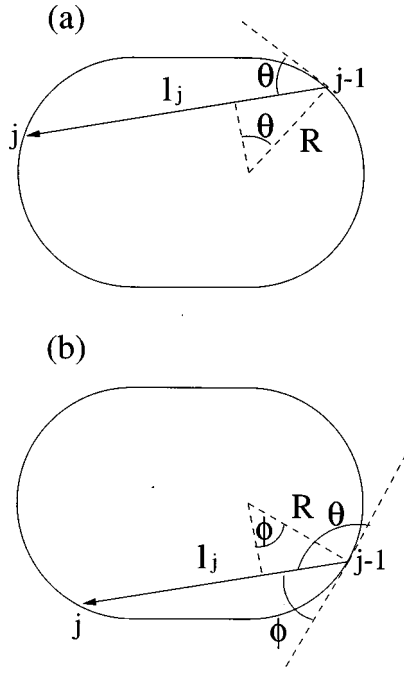


FIG. 1. When the $(j-1)$ th bounce and the j th bounce occur on different semicircles, (a) $R \sin \theta_{j-1} < l_j$ and (b) $R \sin \theta_{j-1} = R \sin(\pi - \theta_{j-1}) = R \sin \phi < l_j$.

point lands on the boundary for a circle billiard or a semicircle side of a stadium is derived. In Sec. IV we make some concluding remarks.

II. A SIMPLE RULE FOR COUNTING CONJUGATE POINTS WHEN ORBITS BEGIN ON THE STADIUM BOUNDARY

We now consider an orbit that starts at the boundary of a stadium billiard. The stadium boundary is composed of four sides, two curved sides of radius R and two straight sides of length W , which can be identified as $N = 1, 2, 3$, or 4 . Let us consider when the orbit has undergone n bounces. For any bounce point of this orbit, we denote the side hit at the j th bounce as N_j , where $0 \leq j \leq n$. Let us denote the elements of \hat{M}_j as \hat{m}_{kl} ($k, l = 1, 2$). We examine the signs of \hat{m}_{kl} . In general, if the $(j-1)$ th bounce occurs on a semicircle with $R_{j-1} = R$, then $a_{j-1} \equiv R_{j-1} \sin \theta_{j-1}$ gives the projection of the radius of the semicircle containing the $(j-1)$ th bounce point onto the line l_j . Similarly, if the j th bounce lands on a semicircle with $R_j = R$, then $a_j \equiv R_j \sin \theta_j$ gives the projection of the radius the semicircle containing the j th bounce point onto the line l_j . We illustrate this in Fig. 1. Since the Birkhoff angle θ is within the range $(0, \pi)$, we have $\sin \theta > 0$ and $\hat{m}_{12} < 0$.

Next we consider the sign of \hat{m}_{11} . For $R_{j-1} = \infty$, we have $\hat{m}_{11} < 0$. For $R_{j-1} = R_j = R$, if the two bounces occur on the same semicircle, $l_j = 2R \sin \theta_{j-1}$ and $\hat{m}_{11} > 0$. If the two bounces occur on different semicircles, we obviously have $l_j > a_{j-1}$. Thus, again, $\hat{m}_{11} > 0$. Similarly, $\hat{m}_{11} > 0$ if $R_{j-1} = R$ and $R_j = \infty$.

Next we consider the sign of \hat{m}_{21} . If both R_{j-1} and R_j are ∞ , $\hat{m}_{21} = 0$. But if only one of them is ∞ , $\hat{m}_{21} > 0$. If

$R_{j-1} = R_j = R$ and $N_{j-1} \neq N_j$, then $l_j < a_{j-1} + a_j$ and $\hat{m}_{21} < 0$. If $R_{j-1} = R_j = R$ and $N_{j-1} = N_j$, then $\hat{m}_{21} = 0$.

Finally, we find $\hat{m}_{22} < 0$ if $R_j = \infty$, but $\hat{m}_{22} > 0$ if $R_j = R$. Collecting the above, we have the following characteristics for signs (+ for greater than zero and - for less than zero) of the elements of \hat{M}_j :

$$\hat{M}_j = \begin{pmatrix} - & - \\ + & + \end{pmatrix} \quad \text{for } R_{j-1} = \infty, R_j = R \quad (3a)$$

$$\hat{M}_j = \begin{pmatrix} - & - \\ 0 & - \end{pmatrix} \quad \text{for } R_{j-1} = \infty, R_j = \infty \quad (3b)$$

$$\hat{M}_j = \begin{pmatrix} + & - \\ + & - \end{pmatrix} \quad \text{for } R_{j-1} = R, R_j = \infty \quad (3c)$$

$$\hat{M}_j = \begin{pmatrix} + & - \\ - & + \end{pmatrix} \quad \text{for } R_{j-1} = R_j = R, N_{j-1} \neq N_j \quad (3d)$$

$$\hat{M}_j = \begin{pmatrix} + & - \\ 0 & + \end{pmatrix} \quad \text{for } R_{j-1} = R_j = R, N_{j-1} = N_j. \quad (3e)$$

Now let us consider the monodromy matrix after n bounces and denote the (k, l) component of $M^{(n)}$ as $m_{kl}^{(n)}$. We prove the following properties associated with the orbit for any $n \geq 1$.

(i) If $R_0 = \infty$ and if there exists a j with $R_j \neq \infty$ ($1 \leq j \leq n$), then $m_{11}^{(n)} m_{12}^{(n)} > 0$ and $m_{21}^{(n)} m_{22}^{(n)} > 0$.

(ii) If $R_j = \infty$ for all j 's ($0 \leq j \leq n$), then $m_{11}^{(n)} m_{12}^{(n)} > 0$ and $m_{21}^{(n)} = 0$.

(iii) If $R_0 = R$ and there exists a j ($1 \leq j \leq n$) with $N_j \neq N_0$, then $m_{11}^{(n)} m_{12}^{(n)} < 0$ and $m_{21}^{(n)} m_{22}^{(n)} < 0$.

(iv) If $R_0 = R$ and $N_j = N_0$ for all j 's ($1 \leq j \leq n$), then $m_{11}^{(n)} m_{12}^{(n)} < 0$ and $m_{21}^{(n)} = 0$.

(v) If $R_n = \infty$, then $m_{22}^{(n)} m_{12}^{(n)} > 0$.

(vi) If $R_n = R$, then $m_{22}^{(n)} m_{12}^{(n)} < 0$.

The conditions listed cover all possible cases.

The orbit has either $R_0 = \infty$ or $R_0 = R$. Let us first consider when $R_0 = \infty$. In this case, we need only to prove (i), (ii), (v), and (vi). We shall use the method of Induction to prove them. From Eqs. (3a)–(3e), these properties are satisfied by \hat{M}_1 after the first bounce. Let us assume that they are satisfied by $M^{(n)}$. We examine them if they are satisfied by $M^{(n+1)}$.

First consider the case when $M^{(n)}$ satisfies (i) and (v). There are two possibilities (choose either upper or lower signs)

$$M^{(n)} = \begin{pmatrix} \pm & \pm \\ \pm & \pm \end{pmatrix}. \quad (4)$$

Here we have $R_0 = R_n = \infty$. Application of Eqs. (3a)–(3e) leads to

$$M^{(n+1)} = \begin{pmatrix} \mp & \mp \\ \mp & \mp \end{pmatrix} \quad \text{for } R_{n+1} = \infty, \\ M^{(n+1)} = \begin{pmatrix} \mp & \mp \\ \pm & \pm \end{pmatrix} \quad \text{for } R_{n+1} = R, \quad (5)$$

depending on whether the $(n+1)$ th bounce occurs on a straight side or a curved side.

Next consider when $M^{(n)}$ satisfies (i) and (vi):

$$M^{(n)} = \begin{pmatrix} \pm & \pm \\ \mp & \mp \end{pmatrix}. \quad (6)$$

Here we have $R_0 = \infty$ and $R_n = R$. Applying Eqs. (3a)–(3e) gives

$$M^{(n+1)} = \begin{pmatrix} \pm & \pm \\ \pm & \pm \end{pmatrix} \quad \text{for } R_{n+1} = \infty, \\ M^{(n+1)} = \begin{pmatrix} \pm & \pm \\ \mp & \mp \end{pmatrix} \quad \text{for } R_{n+1} = R. \quad (7)$$

For $R_{n+1} = R$, we obtain the same signs for both $N_n = N_{n+1}$ and $N_n \neq N_{n+1}$.

Finally, consider when $M^{(n)}$ satisfies (ii) and (v):

$$M^{(n)} = \begin{pmatrix} \pm & \pm \\ 0 & \pm \end{pmatrix}. \quad (8)$$

Here we have $R_0 = R_n = \infty$. Applying Eqs. (3a)–(3e) gives

$$M^{(n+1)} = \begin{pmatrix} \mp & \mp \\ 0 & \mp \end{pmatrix} \quad \text{for } R_{n+1} = \infty, \\ M^{(n+1)} = \begin{pmatrix} \mp & \mp \\ \pm & \pm \end{pmatrix} \quad \text{for } R_{n+1} = R. \quad (9)$$

From Eqs. (5), (7), and (9), we see that $M^{(n+1)}$ again has the same properties (i), (ii), (v), and (vi). Thus, by induction, they are valid for all $n \geq 1$ when $R_0 = \infty$.

We next consider the other case, $R_0 = R$. Here we need to verify (iii)–(vi). Equations (3a)–(3e) show that they are satisfied for the first step $M^{(1)}$. Let us assume that they are satisfied by $M^{(n)}$. We examine if they are satisfied by $M^{(n+1)}$.

First consider the case when $M^{(n)}$ satisfies (iii) and (v). We have

$$M^{(n)} = \begin{pmatrix} \pm & \mp \\ \pm & \mp \end{pmatrix}. \quad (10)$$

Here we have $R_0 = R$ and $R_n = \infty$. Application of Eqs. (3a)–(3e) leads to

$$M^{(n+1)} = \begin{pmatrix} \mp & \pm \\ \mp & \pm \end{pmatrix} \quad \text{for } R_{n+1} = \infty, \\ M^{(n+1)} = \begin{pmatrix} \mp & \pm \\ \pm & \mp \end{pmatrix} \quad \text{for } R_{n+1} = R. \quad (11)$$

Next consider when $M^{(n)}$ satisfies (iii) and (vi):

$$M^{(n)} = \begin{pmatrix} \pm & \mp \\ \mp & \pm \end{pmatrix}. \quad (12)$$

Here we have $R_0 = R_n = R$. Applying Eqs. (3a)–(3e) gives

$$M^{(n+1)} = \begin{pmatrix} \pm & \mp \\ \pm & \mp \end{pmatrix} \quad \text{for } R_{n+1} = \infty,$$

$$M^{(n+1)} = \begin{pmatrix} \pm & \mp \\ \mp & \pm \end{pmatrix} \quad \text{for } R_{n+1} = R. \quad (13)$$

In the case of $R_{n+1} = R$, we obtain the same signs for both $N_n = N_{n+1}$ and $N_n \neq N_{n+1}$.

Finally, consider when $M^{(n)}$ satisfies (iv) and (vi):

$$M^{(n)} = \begin{pmatrix} \pm & \mp \\ 0 & \pm \end{pmatrix}. \quad (14)$$

Here we have $R_0 = R_n = R$. Applying Eq. (3a) gives

$$M^{(n+1)} = \begin{pmatrix} \pm & \mp \\ \pm & \mp \end{pmatrix} \quad \text{for } R_{n+1} = \infty, \quad (15a)$$

$$M^{(n+1)} = \begin{pmatrix} \pm & \mp \\ \mp & \pm \end{pmatrix} \quad \text{for } R_{n+1} = R, \quad N_n \neq N_{n+1}, \quad (15b)$$

$$M^{(n+1)} = \begin{pmatrix} \pm & \mp \\ 0 & \pm \end{pmatrix} \quad \text{for } R_{n+1} = R, \quad N_n = N_{n+1}. \quad (15c)$$

From Eqs. (11), (13), and (15a)–(15c), we see that $M^{(n+1)}$ again has the same properties (iii)–(vi). Thus, by induction, they are valid for all $n \geq 1$ when $R_0 = R$. Collecting these results and the results for $R_0 = \infty$, we have proved that the properties (i)–(vi) are satisfied for all $n \geq 1$.

From these properties, we note that, since $m_{12}^{(n)} \neq 0$, a conjugate point can never happen on the boundary. Obviously, there is no conjugate point between the starting point and the first bounce, independent of whether or not the starting point is on the boundary.

Now let us examine under what conditions there is a conjugate point between the n th bounce and $(n+1)$ th bounce ($n \geq 1$). Since trajectories are straight between bounces, there can be at most one conjugate point. It then follows that, due to the sense of s , if $m_{12}^{(n)} m_{12}^{(n+1)} < 0$, two orbits starting from the same point on the boundary with an infinitesimal difference in angles do not intersect between the n th and the $(n+1)$ th bounce. Hence there is no conjugate point between the two bounces. On the other hand, if $m_{12}^{(n)} m_{12}^{(n+1)} > 0$, the two orbits would have intersected between the two bounces and there is a conjugate point at the intersection [19].

From Eqs. (4)–(15) above, we obtain Table I, which gives signs of $m_{12}^{(n)} m_{12}^{(n+1)}$ for all possible combinations of R_0 , R_n , and R_{n+1} . This table proves that for any $n \geq 1$, there is a conjugate point between the n th bounce and $(n+1)$ th bounce if and only if the n th bounce occurs on a curved side ($R_n = R$). We illustrate this rule in Fig. 2.

A circle billiard is obtained by shrinking the straight sides of the stadium down to zero. Evidently, Table I applies to a circle too, with $R_0 = R_n = R_{n+1} = R$. Hence we have also proved that, for a circle, if the starting point is on the boundary, conjugate points can never land on the boundary and there is a conjugate point after every bounce.

TABLE I. Signs of $m_{12}^{(n)}m_{12}^{(n+1)}$. A plus sign indicates that a conjugate point exists between the n th bounce and the $(n+1)$ th bounce. A minus sign indicates that no conjugate point exists between the two bounces.

R_0	R_n	R_{n+1}	$\text{sgn}(m_{12}^{(n)}m_{12}^{(n+1)})$
∞	∞	∞	-
∞	∞	R	-
∞	R	∞	+
∞	R	R	+
R	∞	∞	-
R	∞	R	-
R	R	∞	+
R	R	R	+

III. EXCEPTIONS TO THE SIMPLE RULE WHEN ORBITS DO NOT BEGIN ON THE STADIUM BOUNDARY

Let us now see what happens when the orbit starts from the interior of a stadium or a circle instead of from the boundary. A practical example of this situation appears in semiclassical calculations of conductance in ballistic quantum dot [10], where a lead is attached on a curved side and trajectories start from the straight junction between the lead and the dot. We shall see that the simple rule of the preceding section is no longer valid. To illustrate this, we consider whether there is a conjugate point after the first bounce if it occurs on a curved side. To aid our analysis, it is possible to insert a fictitious straight side over the starting point without affecting a pencil of trajectories starting from the same point. As we shall see, as long as we are concerned with locations of conjugate points before the orbit hits the fictitious side again, the result of our analysis will be independent of the angle of this straight side. This straight side together with part of the real boundary again forms a new convex billiard system.

Thus we have, by Eq. (1) with $R_0 = \infty$ and $R_1 = R$,

$$M^{(1)} = \begin{pmatrix} \frac{\sin \theta_0}{\sin \theta_1} & \frac{-l_1}{\sin \theta_0 \sin \theta_1} \\ \frac{\sin \theta_0}{R} & \frac{l_1/R - \sin \theta_1}{\sin \theta_0} \end{pmatrix}. \quad (16)$$

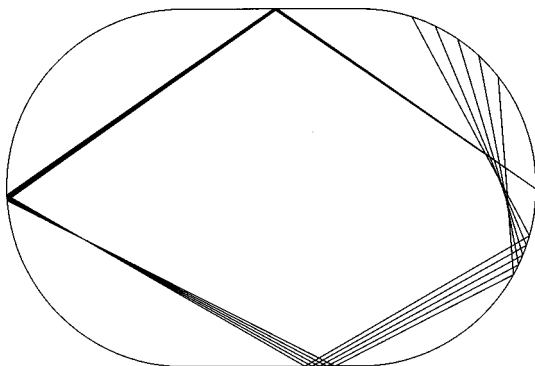


FIG. 2. For an orbit starting from the boundary of a stadium, there is a conjugate point after a bounce off the boundary if and only if the bounce occurs on a curved side.

To simplify the matter, we consider the case of a circle or when both the first and second bounces occur on the same semicircle in the case of a stadium. Then we have $\theta_1 = \theta_2$ and $l_2 = 2R \sin \theta_1$. \hat{M}_2 is simplified to

$$\hat{M}_2 = \begin{pmatrix} 1 & \frac{-2R}{\sin \theta_1} \\ 0 & 1 \end{pmatrix}. \quad (17)$$

These give

$$m_{12}^{(2)} = \frac{l_2 - 3l_1}{\sin \theta_0 \sin \theta_1}. \quad (18)$$

It predicts that if $l_1 < l_2/3$, there is no conjugate point between the first and the second bounces: If $l_1 = l_2/3$, there is a conjugate point on the boundary at the second bounce and if $l_1 > l_2/3$, there is a conjugate point between the first and the second bounces. These are confirmed by direct numerical propagations of a pencil of trajectories starting from the same point inside the boundary as illustrated in Fig. 3. The above presents an explicit rule for the absence of a conjugate point after hitting a curved side and before the next bounce [20].

We see in Fig. 3 that by changing only the starting point of the orbit while allowing it to traverse the same path, it is possible to change the locations of the conjugate points. As l_1 approaches $l_2/3$, a conjugate point moves closer to the boundary. So does the caustic arising from the pencil of trajectories. On the other hand, there is another type of caustic [21], which is the envelop of a “single” trajectory, as shown in Fig. 4. It forms a circle. We shall refer to this type of caustic as a *single-trajectory caustic* and the caustic arising from the pencil of trajectories as a *pencil caustic*. While the three central trajectories of Figs. 3(a)–3(c) all have the same single-trajectory caustic, they have different pencil-caustic structures. Conjugate points in general do not reside on the single-trajectory caustic. What we have shown here clearly demonstrates that the two types of caustics are different and a proper distinction should be made to avoid confusion.

In the case of a stadium, we find that it is not only possible that no conjugate point exists after hitting a curved side as shown in Figs. 5(a) and 5(b); it is also possible that a conjugate point exists after hitting a straight side, as shown in Fig. 5(b). In Fig. 5(b) we have $R_1 = R$, $R_2 = \infty$, and $R_3 = R$. We obtain

$$m_{12}^{(2)} = \frac{-2l_1 l_2 + R \sin \theta_1 (l_1 + l_2)}{R \sin \theta_0 \sin \theta_1 \sin \theta_2} \quad (19)$$

and

$$m_{12}^{(3)} = \frac{2l_1(l_2 + l_3) - R \sin \theta_1 (l_1 + l_2 + l_3)}{R \sin \theta_0 \sin \theta_1 \sin \theta_3}. \quad (20)$$

For the central trajectory of Fig. 5(b) ($R = 1$), $\theta_1 \approx 1.376$, $l_1 \approx 0.366$, $l_2 \approx 1.233$, and $l_3 \approx 2.131$. These give $m_{12}^{(2)} > 0$ and $m_{12}^{(3)} > 0$. It predicts no conjugate point after the first bounce and a conjugate point after the second bounce, consistent with the figure.

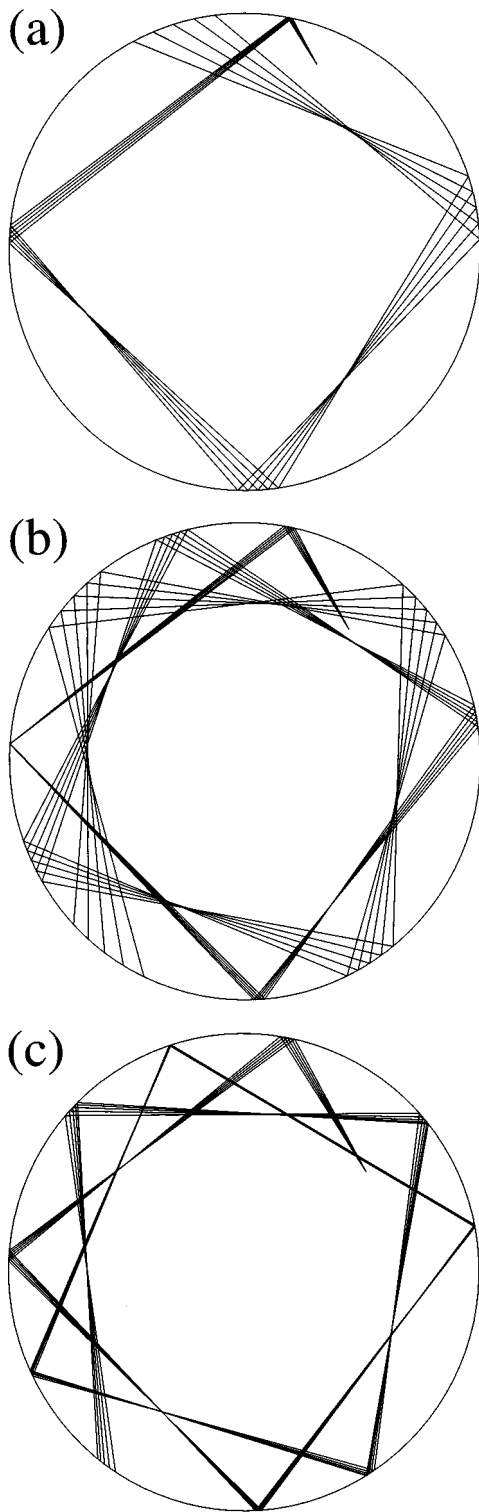


FIG. 3. Pencil of trajectories starting from inside the circle. All the central trajectories in (a), (b), and (c) traverse the same path: (a) $l_1 < l_2/3$, there is no conjugate point between the first and the second bounces; (b) $l_1 = l_2/3$, there is a conjugate point on the boundary at the second bounce and afterward the simple rule in Sec. II applies; (c) $l_1 > l_2/3$, there is a conjugate point between the first and the second bounces. We find that the distance from the conjugate point between the third and the fourth bounces to the fourth bounce is less than l_5 . Consequently, there is no conjugate point between the fourth and the fifth bounces.

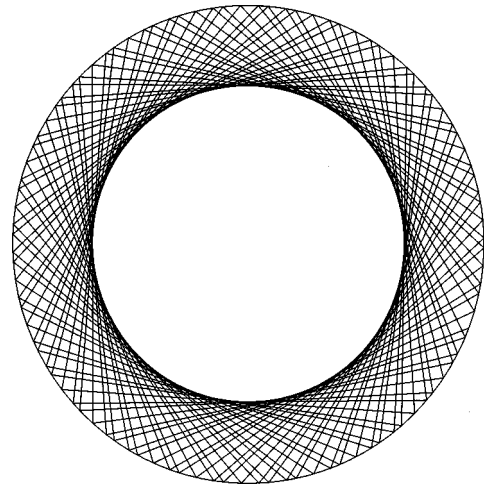


FIG. 4. Long propagation of the central orbit of Fig. 3(b). The inner circle, concentric with the circular billiard boundary, forms the caustic of the “single” trajectory. Every cord is tangent to the caustic circle. Thus it touches the caustic at the midpoint.

IV. CONCLUSION

In this paper we have proved that by propagating the orbit starting from the boundary of a stadium or a circle billiard, a simple rule for counting the conjugate points encountered by the orbit is obtained. Thus, for semiclassical calculations that require summations over orbits that begin and end on the boundary, it simplifies the calculation of the Maslov index

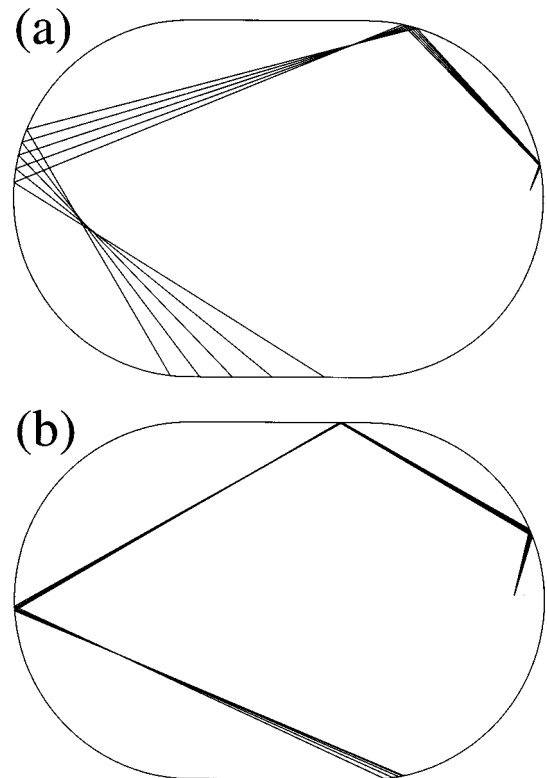


FIG. 5. (a) Since $l_1 < l_2/3$, there is no conjugate point between the first and the second bounces. (b) There is no conjugate point between the first and the second bounces. The second bounce occurs on a straight side and there is a conjugate point between the second and the third bounces.

for stadium and circle billiards. It also allows analytical derivation of the phase associated with the orbit in the case of a circle billiard.

The simple rule of one conjugate point after every curved side hit if the orbit starts from the boundary provides an unambiguous assignment of the Morse index α (the total number of conjugate points encountered by the orbit) for the symbolic code of a trajectory in terms of a sequence of different sides hit [22], $\alpha = n_c$, where n_c is the total number of times a curved side was hit. The connection between classical indices (such as the Morse index or Maslov index) and symbolic coding of trajectories has been discussed by Eckhardt and Wintgen [23]. Here we have provided another example of such a connection. The correspondence between symbolic coding of classical trajectories in the quadratic Zeeman effect and the four-disk billiard problem [23] suggests that such a connection may be extended to the soft-wall

stadium, studied by Tomsovic and Heller [9].

We have also proved that conjugate points can never land on the boundary if the orbit starts from the boundary. If orbits contributing to a semiclassical sum (such as the Gutzwiller trace formula [13]) depend only on paths but not starting points (such as periodic orbits), a simple way to avoid a conjugate point (where the semiclassical approximation breaks down) is to start the orbit from the boundary. By contrast, if orbits begin from the interior of the billiard domain, it might not be so easy to avoid the conjugate points for all the orbits, especially when the number of orbits needed to be included in the sum is large.

ACKNOWLEDGMENT

This research was supported by the NSF (Grant Nos. PHY-9214816 and PHY-9507574).

-
- [1] R. A. Jalabert, H. U. Baranger, and A. D. Stone, *Phys. Rev. Lett.* **65**, 2442 (1990).
- [2] R. V. Jensen, *Chaos* **1**, 101 (1991).
- [3] C. M. Marcus, A. J. Rimberg, R. M. Westervelt, P. F. Hopkins, and A. C. Gossard, *Phys. Rev. Lett.* **69**, 506 (1992); C. M. Marcus, R. M. Westervelt, P. F. Hopkins, and A. C. Gossard, *Chaos* **3**, 643 (1993).
- [4] H. U. Baranger, R. A. Jalabert, and A. D. Stone, *Phys. Rev. Lett.* **70**, 3876 (1993); *Chaos* **3**, 665 (1993).
- [5] W. A. Lin, J. B. Delos, and R. V. Jensen, *Chaos* **3**, 655 (1993).
- [6] A. M. Chang, H. U. Baranger, L. N. Pfeiffer, and K. W. West, *Phys. Rev. Lett.* **73**, 2111 (1994).
- [7] E. B. Bogomolny, *Physica D* **31**, 169 (1988).
- [8] S. C. Creagh, J. M. Robbins, and R. G. Littlejohn, *Phys. Rev. A* **42**, 1907 (1990).
- [9] S. Tomsovic and E. J. Heller, *Phys. Rev. E* **47**, 282 (1993).
- [10] W. A. Lin and R. V. Jensen, *Phys. Rev. B* **53**, 3638 (1996).
- [11] C. D. Schwieters, J. A. Alford, and J. B. Delos, *Phys. Rev. B* **54**, 10 652 (1996).
- [12] W. A. Lin, *Chaos Solitons Fractals* **8**, 995 (1997).
- [13] M. C. Gutzwiller, *Chaos in Classical and Quantum Mechanics* (Springer-Verlag, New York, 1991).
- [14] M. C. Gutzwiller, *J. Math. Phys.* **8**, 1979 (1967); **12**, 343 (1971).
- [15] M. V. Berry, *Eur. J. Phys.* **2**, 91 (1981). An independent derivation of this matrix can be found in Ref. [12].
- [16] G. D. Birkhoff, *Acta Math.* **50**, 359 (1927).
- [17] J. D. Meiss, *Rev. Mod. Phys.* **64**, 795 (1992).
- [18] R. G. Littlejohn, *Rev. Mod. Phys.* **31**, 2952 (1990).
- [19] Instead of the Birkhoff coordinates used here, one can also use a local coordinate system associated with the orbit to compute the monodromy matrices. Then, if the sign of the 1-2 component of the monodromy matrix for n bounces is opposite that for $n+1$ bounces, then there is a conjugate point between the two bounces [8,9].
- [20] However, it has been shown previously that the number of conjugate points encountered in a periodic orbit of a stadium depends on the starting point [8]. In Fig. 6(a) of that paper, for a periodic orbit of a stadium, no conjugate point was encountered after the fourth bounce, which lands on a curved side, since the orbit completes the period. But allowing further propagation beyond the period, the orbit will go through a conjugate point before the next bounce.
- [21] This is the type of caustic that is often defined in mathematical literatures. See, for example, V. V. Kozlov and D. V. Treshchëv, *Billiards* (American Mathematical Society, Providence, 1991), p. 142.
- [22] O. Biham and M. Kvale, *Phys. Rev. A* **46**, 6334 (1992).
- [23] B. Eckhardt and D. Wintgen, *J. Phys. B* **23**, 355 (1990); *J. Phys. A* **24**, 4335 (1991).